**THE EUROPEAN**
**PHYSICAL JOURNAL D**

Regular Article – Optical Phenomena and Photonics

# Stimulated Brillouin scattering in an inhomogeneous amplifier cell: a self-consistent solution approach

M. Jaberi[1,a] and S. Panahibakhsh[2,b]

[1] Plasma and Fusion Research School, Nuclear Science and Technology Research Institute, Tehran, Iran
[2] Photonics and Quantum Technologies Research School, Nuclear Science and Technology Research Institute, Tehran, Iran

**Abstract.** In this paper, the amplification of the injected Stokes wave in inhomogeneous media has been studied. Numerical calculations based on a self-consistent solution of the Maxwell equations for the electric fields and the Navier–stokes equation for the acoustic fields are used to explain the amplification of the Stokes waves. To consider inhomogeneous media, the SBS amplifier cell is divided into several parts by transparent thin surfaces with uniform density distribution. This process was applied to several configurations of SBS gain factor changes in the cell, including exponential and linear changes in Brillouin gain factor according to the subdivision within the cell, and the results were compared. The results show that the length of the medium plays an essential role in the growth of SBS performance. Also, by the optimum selection of the gain profile, a non-uniform gas pressure distribution in the SBS cell can improve the energy reflectivity and the optical breakdown threshold.

## 1 Introduction

In recent decades, Stimulated Brillouin scattering has resulted in high-efficiency phase conjugate back scattered mirrors (PCM) production [1–6]. An interesting application of PCM is the correction of the aberrations caused by optical elements in the system that would improve beam quality and performance of high-power lasers over wide laser wavelength ranges. [7–14]. PCM of laser beam based on the SBS is used to pulse compression by backward-wave amplification [15–22], slow light [23–25], Orbital angular momentum (OAM) [26, 27], Brillouin spectroscopy[28, 29], microscopic imaging [30] and beam combinations [31–35].

Some important parameters that characterize the Brillouin Scattering efficiency are material parameters such as steady state gain coefficient ($g_B$), acoustic decay time ($\tau_B$), acoustic velocity ($\nu_B$), and also cell configurations such as focused single cell, compact generator-Amplifier cell [36–40] and cell length [6, 20]. SBS has been observed in pressurized gases in many applications [41–45]. The high-pressure gases are preferred as SBS gain media in phase conjugation because of their optical quality and low-frequency Shifts. Also, due to their high transparency throughout the ultraviolet to infrared regions of the electromagnetic spectrum are very attractive. By increasing the pressure

(and hence density) of the gas, very high gain coefficients can be achieved, although the decay time of the sound increases.

At high laser powers, the high-pressure homogeneous gasses can limit the SBS performance due to low optical breakdown threshold and high absorption rate. Both can result in decreasing the SBS performance in terms of PC fidelity, stability, and energy reflectivity (ER) or Energy conversion efficiency. Also, the optical breakdown can occur in the low threshold high-pressure gas when the pump is strong. On the other hand, in low-power systems that require a high Brillouin gain, it is preferable to use a medium with a short acoustic decay time ($\tau_B$) for work with short pulses [45].

In most theoretical and experimental research, the homogenous (uniform) medium in the SBS cells has been demonstrated. In this paper, we introduce a method to investigate the SBS process in a non-uniform media and compare it with a uniform one. Compressed xenon gas was selected because of its superior optical qualities, high SBS gain, and small stokes shifts. Xenon is a well-known SBS medium that has been characterized and many of its important parameters had been investigated [45, 46]. Also, a two-cell system was considered in which the generator cell has a uniform gas distribution, while the amplifier cell has a non-uniform xenon gas distribution at a pressure between 1 and 50 (atm) and was seeded by a phase-conjugated stokes beam of the generator cell. The calculations are concentrated on the amplifier cell. Two approaches were considered for the amplifier cell. First, the non-uniform distribution

[a] e-mail: mohammad.jaberi@gmail.com (corresponding author)

[b] e-mail: panahi.spb@gmail.com

within the cell was produced by dividing the cell into several subdivision parts with uniform density distribution,

Second, the length of the SBS cell was changed as an important parameter in geometrical factors to obtain maximum energy reflectivity. This procedure was applied to several configurations of SBS gain factor changes in the cell, including exponential and linear changes in gain factor according to the subdivision within the cell, and the results were compared.

It was found that the SBS performance could be improved by the choice of the non-uniform medium in the amplifier cell. In addition, it was found that choosing the type of inhomogeneity inside the cell makes another advantage, such as increasing the optical breakdown threshold inside the cell by increasing the pump energy, and also in low pressure that the phonon lifetime is small, it allows the use of short laser pulses in the steady state.

## 2 Numerical method

To describe the SBS process the equations derived from the Maxwell equations for the electric fields and Navier–stokes equation for the acoustic fields are used. By using the slowly varying envelope approximation (SVEA) for the electric and acoustic fields, the description of the incident and reflected light waves and their coupling to the sound wave is simplified, i.e., the amplitude of the fields is assumed to vary slowly in time ($t$) and space ($z$) as compared with their temporal and spatial frequencies. Transverse field variations are neglected. The SBS equations describing the acoustic, Stokes, and pump field propagating along the z direction are given as:

$$\frac{n}{c}\frac{\partial E_p}{\partial t} + \frac{\partial E_p}{\partial z} + \frac{1}{2}\alpha E_p = ig_1 E_s \rho$$
$$\frac{n}{c}\frac{\partial E_S}{\partial t} - \frac{\partial E_S}{\partial z} + \frac{1}{2}\alpha E_S = ig_1 E_p \rho^*$$
$$\frac{\partial \rho}{\partial t} + \frac{\Gamma_{\mathrm{B}}}{2}\rho = ig_2 E_p E_S^* \tag{1}$$

where the derivative in transverse directions $x$ and $y$ are neglected, $g_1$ and $g_2$ are coupling constants given by

$$g_1 = \frac{w_L}{4nc}\frac{\gamma_e}{\rho}$$

$$g_2 = \frac{\gamma_e \varepsilon_0 K_{\mathrm{B}}}{4v}$$

$\rho$ denotes the density of the nonlinear medium and $v$ represents the velocity of the acoustic waves. $\gamma_e$ and $n$ are the electrostrictive coefficient and the refractive index, respectively. $c$ is the speed of light and $\Gamma_{\mathrm{B}}$ is the SBS spontaneous bandwidth equal to the inverse of the acoustic lifetime $\tau_{\mathrm{B}}$.

By introducing the following conditions:

$$\frac{\gamma_e}{2cn}(I_p I_s)^{\frac{1}{2}} \gg \rho v^2, \frac{\partial \rho}{\partial t} \ll \frac{\Gamma_{\mathrm{B}}}{2}\rho$$

Equation (1) becomes

$$\frac{n}{c}\frac{\partial I_p}{\partial t} + \frac{\partial I_p}{\partial z} = -\alpha I_p - g_{\mathrm{B}} I_p I_s, \frac{n}{c}\frac{\partial I_s}{\partial t} - \frac{\partial I_s}{\partial z}$$
$$= -\alpha I_s + g_{\mathrm{B}} I_p I_s \tag{2}$$

where $\alpha$ is the linear optical loss in the material, $I_p$ and $I_S$ are the pump and stokes intensity at the entrance of the cell, and $g_{\mathrm{B}} = \frac{\omega_p^2 \gamma_e^2 \tau_{\mathrm{B}}}{c^3 nv\rho_0}$ is the optical gain associated with the SBS process. In these equations the intensity depleted and medium absorption is considered. Let us consider a single longitudinal mode laser pulse with length $l_P$ corresponding to the pulse width $t_p$, and the phonon lifetime in nonlinear media is $\tau_{\mathrm{B}}$. The maximum interaction length between the optical and acoustic fields within the nonlinear medium is $l_c$ and defines the characteristic length:

$$l_c = \left\{ \begin{array}{l} \frac{ct_p}{n}, t_p < \tau_{\mathrm{B}} \\ \frac{c\tau_{\mathrm{B}}}{n}, t_p > \tau_{\mathrm{B}} \end{array} \right\}$$

The definition of $l_c$ is related to the interaction time of the pump and acoustical waves. So, the acoustic decay time cause to characterize the Brillouin parameters such as interaction length in the steady state regime ($t_p \gg \tau_{\mathrm{B}}$) and SBS gain coefficient.

To obtain the steady-state solution of presented equations, a self-consistent method is introduced. In this method, we can obtain a steady-state solution for inhomogeneous media that has different gain and absorption coefficients due to changes in gas pressure or density of the media in the cell.

In this paper, the pump laser enters at $Z = 0$ and the injected stokes field enters at $Z = L$ as shown in Fig. 1. The SBS equations in (2) can be solved by a self-consistent iterative procedure. In the SBS amplifier the values of $I_s(L), I_p(0)$ are specified. To find the unknown variable $I_s(0)$, we follow the steps below:

1. An initial guess for $I_s(0)$ is assumed.
2. SBS steady-state equations are calculated based on the guess and initial value of $I_L(0)$ by a normal initial value method.
3. If the difference between the computed value of $I_s(L)_{\mathrm{cal}}$ and the real value of $I_s(L)_{\mathrm{measure}}$ is lesser than the accuracy error, the computation is finished, else:
4. The initial guess value for $I_s(0)$ is repaired by the following equation

$$I_s(0)_{\mathrm{new}} = I_s(0)_{\mathrm{old}} + \beta(I_s(L)_{\mathrm{measure}} - I_s(L)_{\mathrm{cal}})$$

Where $\beta$ is a normal and positive number to prevent diverging computed value $I_s(L)$.
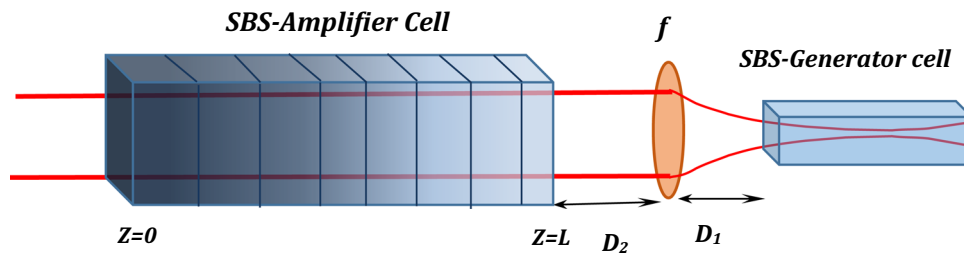
**Fig. 1** Schematic picture of the SBS Amplifier-Generator cells, in this pattern we suppose gas pressure in the Amplifier cell uniformly increases or decrease in the z-direction which is divided into 3 or 11 part by transparent thin surfaces with uniform pressure

5.  Steps 2 to 4 are repeated until step 3 is satisfied. The method can be considered for both the SBS amplifier and the SBS generator systems.

We were particularly attentive to the influence of the non-uniform gain coefficient in the amplifier cell. For this purpose considered an inhomogeneous medium in different Brillouin gain coefficient profiles is described below:

a.  Constant gain coefficient to comparison (uniform pressure).
b.  Non-uniform medium by linear changes in gain coefficient in the $Z$ direction (Fig. 2a,c).
c.  Non-uniform medium by the exponential gain coefficient in the $Z$ direction (Fig. 2a, c).
d.  Different permutations of three selected gain coefficients as a non-uniform environment (g1 g2 g3 (cm/MW)) by equal subdivision length.

The variation of the Brillouin gain coefficient can be explained by changing the gas pressure (and hence density) in the cell, the Xenon gas at a pressure between 1 to 50 atmospheres selected for this purpose.

For obtaining the steady-state solution of the SBS process by the self-consistent method, it is assumed that the cell can be divided into several parts having thin and transparent surfaces with uniform density distribution, hence the non-uniform distribution within the cell can be produced by increasing the number of subdivisions. This method can be considered for both the SBS amplifier and the SBS generator systems. Here, the laser pulse is injected into the system from $z = 0$ whereas, the Stokes pulse is inserted from the last point of the system $(z = L)$ with an intensity lesser than the laser beam $(I_s(L) = 0.05 * I_p(0))$. We assume the laser pulse width equals 30 ns which is larger than the phonon lifetime for Xenon gas, $(\tau_B = 14.6 \text{ ns in} P = 45 \text{atm and } \lambda_p = 694 \text{ nm})$. The SBS cell length was chosen at 140 mm, the laser beam radius is w = 1.6 mm, hence the laser intensity becomes less than the optical breakdown threshold in 694.3 nm wavelength. The material parameters were chosen from Fig. 2a–c for the gain and phonon lifetime, as a function of the pressure of Xenon gas in the cell. In [45], it is given a formula

$\tau_B = 0.65\lambda_p^2 P$ for Xenon gas in which P is in (atm) and laser wavelength $\lambda_p$ is in $(\mu \text{m})$.

## 3 Results and discussion

In this section, the different gain profiles presented in the previous section are investigated and compared. Equations (2) are solved numerically and the obtained results are shown below:

(i) *Selection of constant gain coefficient (uniform pressure) in amplifier cell.*

In this configuration, it is assumed that cell was filled by uniform pressure gas at three selected pressures (29–38-45(atm)). The results are compared with each other. The gain coefficient induced by these pressures is equal to (0.021, 0.041, and 0.061 (cm/MW)), respectively. Figure 3a shows the energy reflectivity (ER) of the selected pressure of gas versus input energy. The result shows that high Brillouin performance in the high gain coefficient and high input power can be extracted. Figure 3b shows the exchange energy of the laser pulse to the Stokes pulse in the medium. The input pump intensity is depleted exponentially, and the Stokes beam grows exponentially up to the input intensity. In this diagram, the input energy is 50 mJ and the cell pressure is 45 atm.

(II), (III) *Non-uniform distribution of gas inside the cell by linear and exponential changes in gain coefficient in the Z direction.*

For this profile of the gas distribution inside the cell, the cell is divided into 11 equal parts by thin and transparent surfaces with the gain coefficient compatible with Fig. 2c. In each section, the xenon gas pressure is uniform and the Brillouin gain increases (decreases) in the entire cell. We assume the first part of the cell, which is beginning from $z = 0$, has the minimum (maximum) gain coefficient.

Our numerical method was applied to this configuration of the SBS cell and the results are plotted in Figs. 4 and 5. The exchange energy of the laser pulse to the Stokes pulse in the medium is shown in Fig. 4. When the gain profile decreases to the minimum value from the beginning part at $z = 0$ to the end part at $z = L$, the input pump intensity is depleted exponentially, and the Stokes beam grows exponentially up to
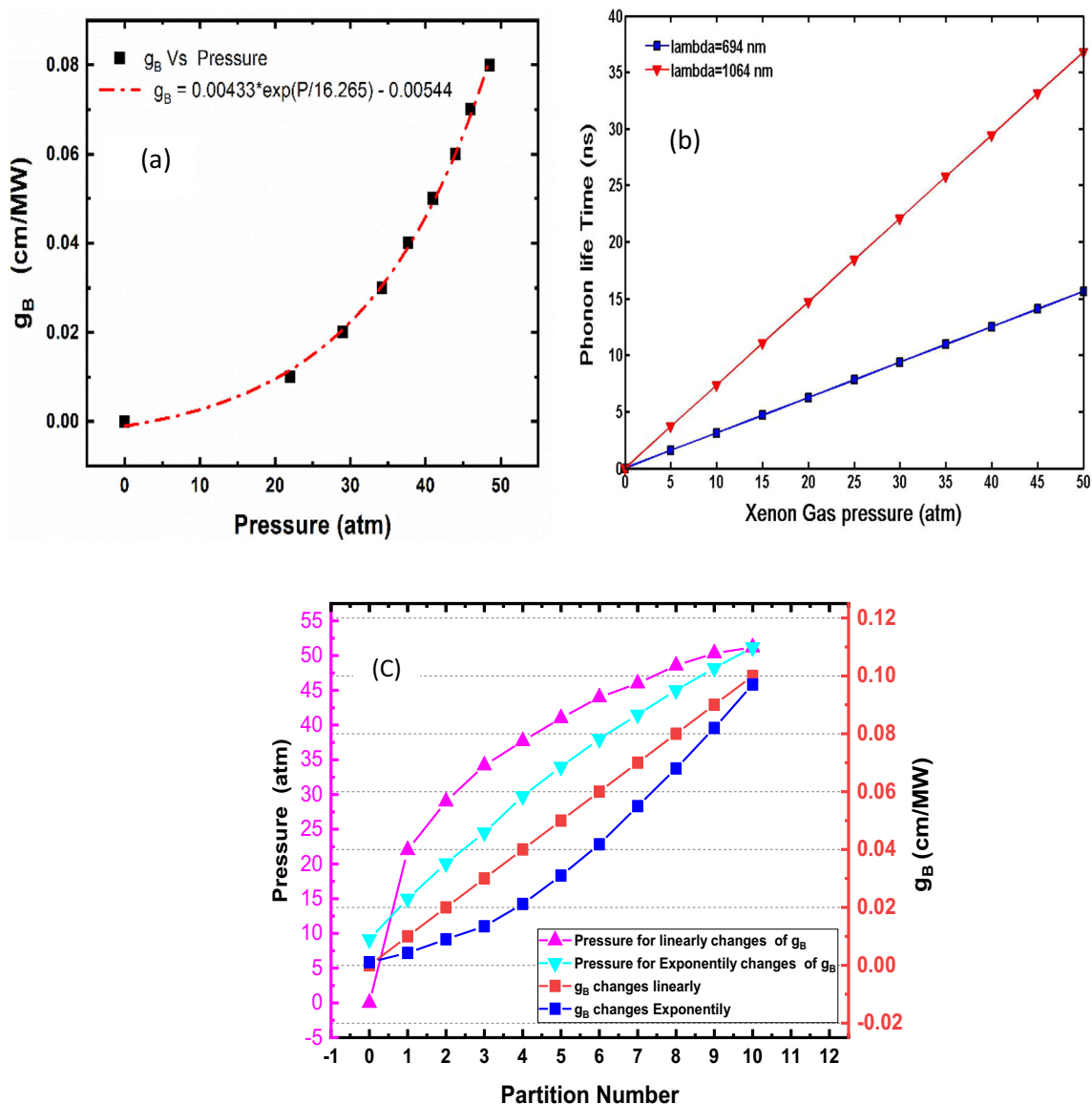
**Fig. 2** (a) Brillouin gain coefficient Profile and (b) Phonon lifetime in $\lambda = 694 nm$ and $1064 nm$ for versus Xenon gas Pressure extracted from experimental setup in [45] (c) The trend of changes in the Brillouin gain according to cell division exponential and linearly is shown along with the corresponding pressure values for comparison

the input intensity. But when the gain profile increases to the maximum pressure in the cell during the partition arrangement, the laser intensity has a low exchange energy to the Stokes pulse because of the low SBS gain value and low acoustic decay time. So the variation of laser and stokes pulse energy in the medium is illustrated in Fig. 4. This trend has the same behavior in both linear and exponential changes of gain coefficient in the cell deviations from each other. In this diagram, the input energy is 50 mJ and the cell pressure is 45 atm.

In this case, we expect that the SBS performance will be changed when the gain value decreases compared to when it increases in the cell. The Energy reflectance of both arrangements of partitions in the cell is depicted

in Fig. 5. The result shows that decreased pressure in the amplifier cell has higher Brillouin performance due to the higher gain and exponential exchange energy between laser and stokes pulse in the entrance of the cell. On the other hand, a low phonon lifetime in the end section of the cell and linearly exchange energy in low stokes amplitude resulted in a decrease in high absorption rate and high stokes energy losses in that part.

In high-power laser systems, the optical breakdown threshold is low when the high-pressure gas is in the cell. So in the focused geometry, the laser power increases at the endpoint of the cell, and the SBS profile discussed above has an advantage in decreasing the
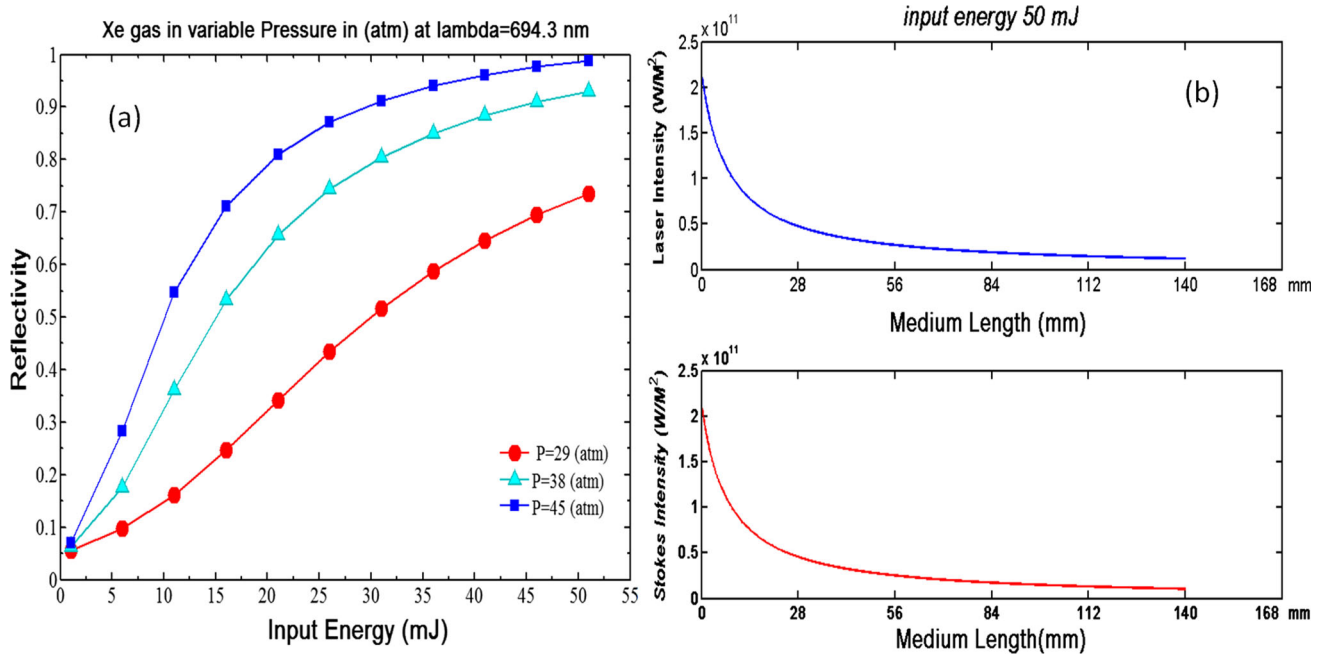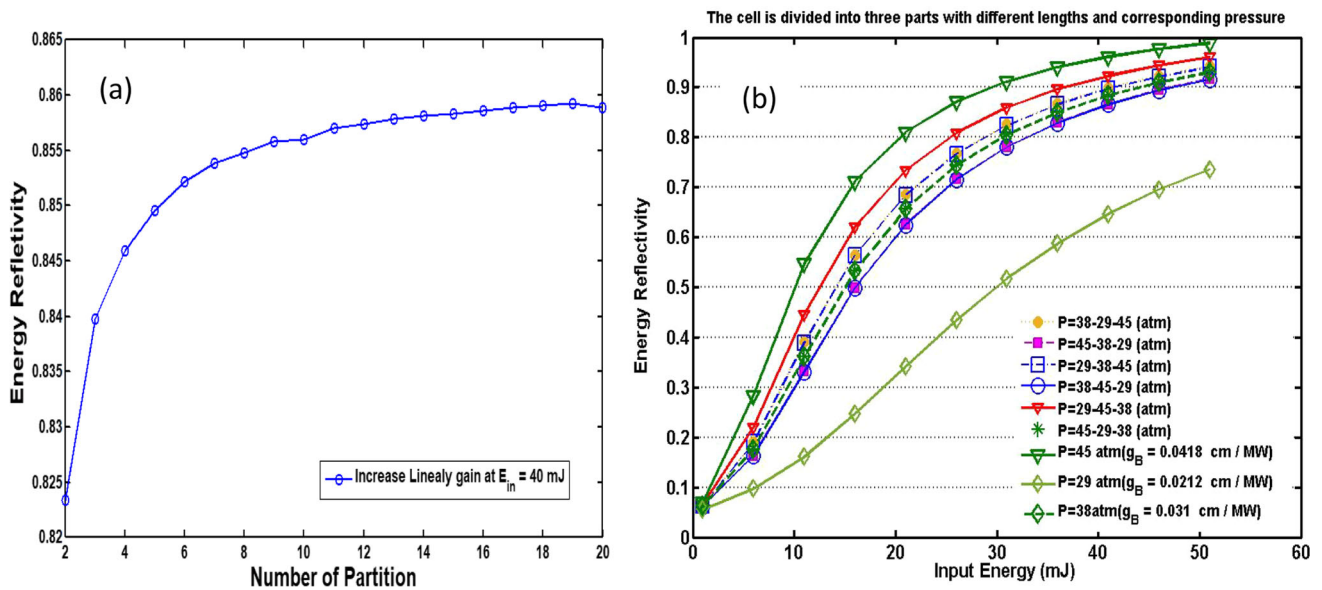
**Fig. 3** (a) Energy reflectivity versus input energy in three selected pressure- b) Changes in the laser and backward Stokes Intensity in the cell length for 50 mJ input energy in 45 atm pressure in the uniform gain coefficient configuration
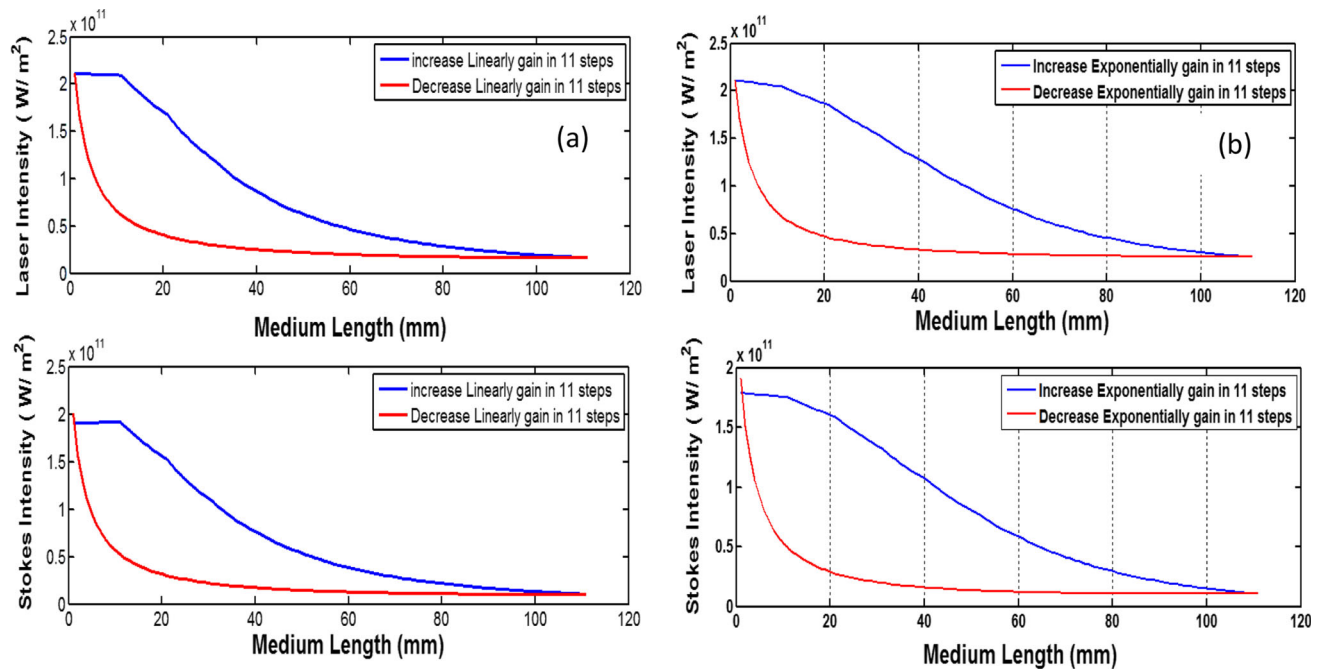


**Fig. 4** The variation of the laser and backward Stokes intensity during the cell when the SBS gain in the medium decreases or increases along the cell length with (a) linear gain profile and (b) exponential gain profile (for 50 mJ input energy is 45 atm)
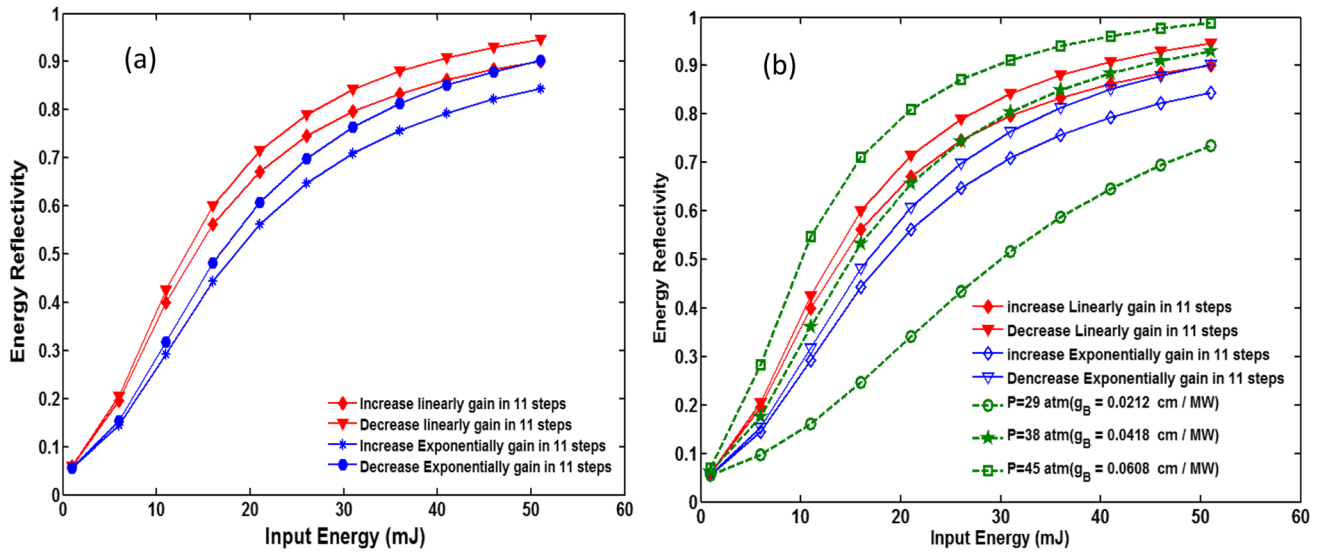
**Fig. 5** Energy reflectance of SBS cell as a function of the incident laser energy for non-uniform distribution of gas inside the cell by linear and exponential changes in gain coefficient in the Z direction as a decrease or increase Brillouin gain coefficient in the cell (b) Comparing Energy reflectivity for Non-uniform distribution of gas inside the cell by uniform distribution of selected pressures



**Fig. 6** (a) The Energy Reflectivity for linear increasing of gain in cell versus the number of partitions at 40 mJ input energy. (b) Energy reflectance of SBS cell as a function of the incident laser Energy for different permutations of three selected gain coefficients by a different length in the last partition as a non-uniform environment (g1 g2 g3) and compare this configuration to the uniform and constant pressure in the cell

optical breakdown that deteriorated the SBS performance in terms of phase conjugate (PC) fidelity, stability, and Energy conversion efficiency. However, the two configurations of SBS gain in the medium have similar behavior, but the linear gain profile in the cell gives higher SBS performance with respect to the exponential change of the gain coefficient in the cell.in Fig. 5a the ER value of both profiles is illustrated. The linear profile of gain in the cell is slightly larger than the other configuration.

In Fig. 5b, the Energy reflectivity for the non-homogeneous distribution of gas inside the cell by linear and exponential changes in gain coefficient are compared with the results of uniform distribution of three selected pressure (29, 38, and 45 atm) whose gain coefficients are (0.021, 0.041, and 0.061 cm/MW), respectively. The result shows that the linear decreases of gain in the cell have higher energy reflectivity with respect to the others except for the uniform pressure in 45 atm,
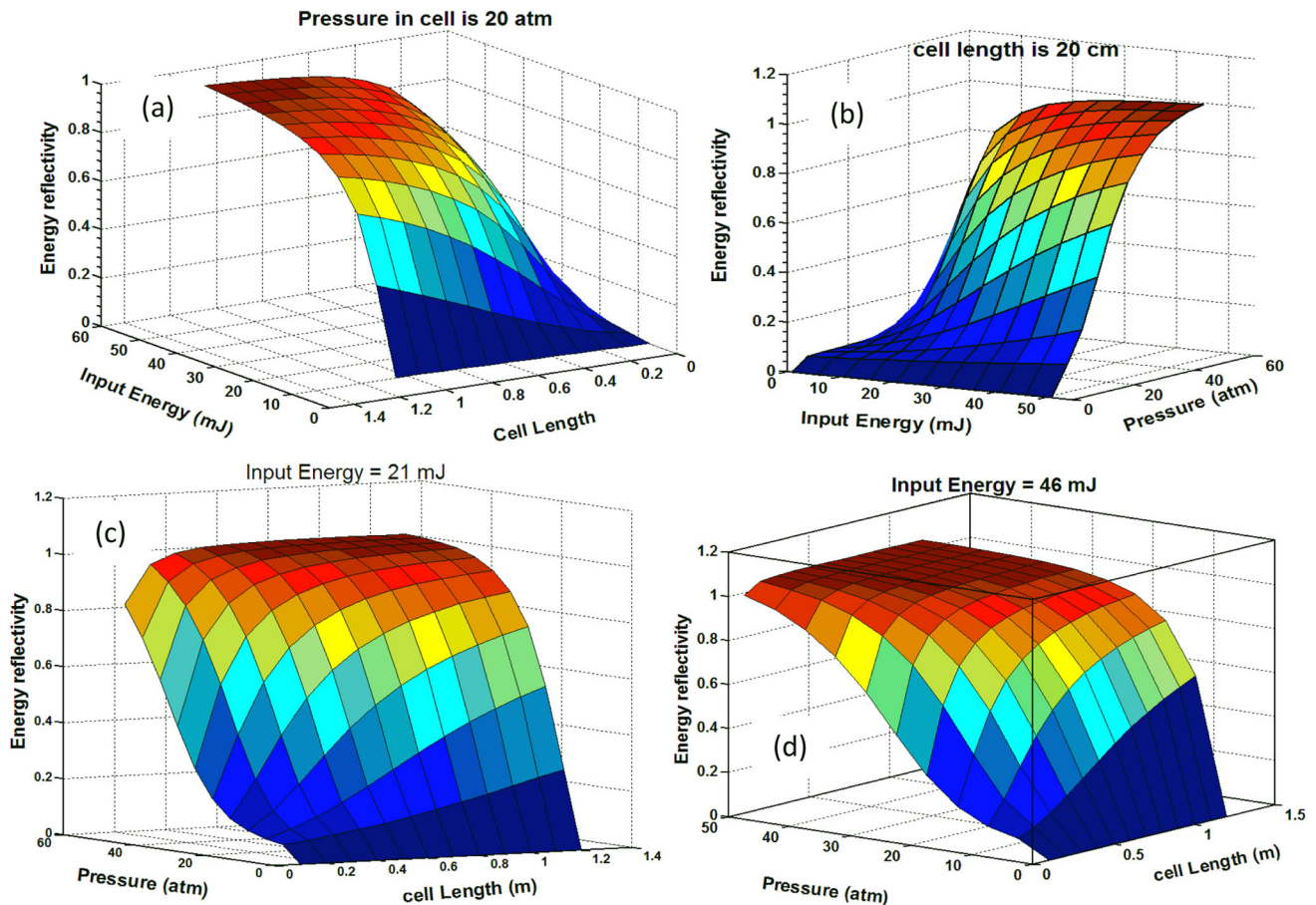
**Fig. 7** Simulation result: distribution of Energy reflectance as a function of (a) cell length and incident laser pulse at pressure 20 atm, (b) cell pressure and incident laser pulse for cell length 20 cm, (c) pressure and length of the cell for the energy of incident laser pulse; 21 mJ and (d) pressure and cell length for the energy of incident laser pulse; 46 mJ, which is higher than 100% when the pressure and cell length are above 30 atm and 40 cm respectively

so the benefits mentioned before (in the below Fig. 4) are confirmed.

The effect of the number of partitions on ER value and comparing them together was studied and the results are shown in Fig. 6a. In this figure, the ER for linear increasing of gain in a cell at 40 mJ input energy versus the number of sub deviations are illustrated. The results show that by increasing the number of partitions the ER increases. The ER in 11 partitions approximately reaches a stationary state, so it is a good election to describe the phenomenon in an unhomogenized medium and compare it to the uniform one.

*(IV)- Different permutations of three selected gain coefficients as a non-uniform environment (g1 g2 g3) by unequal subdivision length.*

Let us consider SBS cell was divided into three partitions with uniform density distribution, filled by xenon gas at three selected pressure (29, 38, and 45 atm) by unequal subdivision lengths whose gain coefficients are (0.021, 0.041, and 0.061 cm/MW), respectively. Hence

we have 6 permutations of three selected gain coefficients. In Fig. 6b the energy reflectivity for these permutations is shown and compared by constant and uniform pressure.

Here, the partition lengths are respectively (40 mm, 40 mm, and 60 mm) to identify the effect of cell length as the end partition size for PC performance. The result shows that all permutations have the same performance approximately and the permutation by $P = 29 - 45 - 38(\text{atm})$, has the maximum value. Furthermore, it is observed the ER is different for some configurations resulting from the changes in the cell length and pressure on Brillouin efficiency. Therefore, one has to change the cell length or the number of partitions to obtain clearer results. In Fig. 6b, the optimal permutations are compared to the configurations having uniform pressure in the whole cell. The results show that the reflected energy obtains a larger value compared to the condition where the cell pressure is equal to the average pressure of the indicated permutations (Approximately 40 atm). In most reports, there are usually deviations between numerical and experimental

results. Due to density changes and sound wave production in the environment due to the electrostriction effect, the deviation between the experiment and simulation can be compensated by considering non-uniform pressure.

As researchers have shown the cell length has an important role to obtain maximum energy reflectivity from the amplifier cell [6, 45], in our consideration we assume that the interaction length $l_c = (c\tau_B)/n$ is varied in interval $\{0$–$1.1$ m$\}$. The dependence of Energy reflectance on pressure and cell Length as a function of the energy of the incident laser pulse is shown in Fig. 7a,b,c. Results show that the ER value increases by increasing cell length, and the slope of ER versus input energy increases.

When the cell length is increased the interaction length of the laser and stocks pulse reaches to characteristic length $l_c$ in the steady-state regime. We found when the length cell is larger than 40 cm, the maximum energy reflectivity in high-pressure reaches a value over 100% (See Fig. 7d), the results that the important parameters that characterize a Brillouin Scattering efficiency are its steady-state gain coefficient ($g_B$), cell length, input energy, and acoustic decay time ($\tau_B$). By increasing the pressure (and hence density) of the gas, it is also possible to achieve very high gain coefficients when the cell length was selected in the optimum value. However, this is accompanied by an increase in the acoustic decay time. In many applications such as SBS pulse compression, the correct choice of optimum length and gas pressure is very important due to their relation to the phonon lifetime (and hence the Brillouin gain) in the medium. Therefore, choosing the optimum length of each part according to its pressure could help to increase the reflectivity of energy and the system's advantage relative to the use of a high-pressure cell with low breakdown energy.

## 4 Conclusion

In this paper, we introduced a method to investigate the SBS process in a non-uniform medium and to compare the SBS performance with the uniform medium. An amplifier SBS cell is considered in which the stokes pulse is injected into the amplifier from the endpoint of the cell. We assume the generator cell has a uniform gas distribution, while the amplifier has a non-uniform gas distribution. The calculations are concentrated on the amplifier cell. This method can be considered for both the SBS amplifier and the SBS generator systems. The results show that the choice of the non-uniform medium in the amplifier cell leads to the improvement of SBS performance. Also, choosing the type of inhomogeneity inside the cell makes other advantages, such as increasing the optical breakdown threshold inside the cell by increasing the pump energy, and allowing the use of a short laser pulse in the steady state in low pressure that the phonon lifetime is small. In addition, by decreasing the pressure from the entrance point to the end

point of the amplifier cell, the reflected energy increases compared to the case where the pressure inside the cell is uniform and equal to the average pressure of the previous state. In this type of non-uniformity of gas in the cell, for the focal geometry and with strong input energy, the threshold of optical breakdown at the end of the cell increases due to the low gas pressure in the selected partition of the cell. Selecting an optimum non-uniformity of gas pressure in the SBS cell can increase the optical breakdown threshold and increase the energy reflectivity, by decreasing the pressure at the focal point of the lens and increasing the pressure at the entrance of the laser to the cell.

## Author contribution

All authors equally contributed to manuscript preparation.

## References

1. E. Garmire, Stimulated Brillouin review: invented 50 years ago and applied today. Int. J. Opt. **2018**, 2459501 (2018)
2. T. Omatsu, H.J. Kong, S. Park, S. Cha, H. Yoshida, K. Tsubakimoto et al., The Current Trends in SBS and phase conjugation. Laser Part. Beams **30**, 117–174 (2012)
3. A. Brignon, J.-P. Huignard, *Phase Conjugate Laser Optics,* vol. 9, Wiley, New York (2004)
4. G.S. He, Optical phase conjugation: principles, techniques, and applications. Prog. Quantum Electron. **26**, 131–191 (2002)
5. Z. Bai, H. Yuan, Z. Liu, P. Xu, Q. Gao, R.J. Williams et al., Stimulated Brillouin scattering materials, experimental design and applications: a review. Opt. Mater. **75**, 626–645 (2018)
6. M. Damzen, V. Vlad, A. Mocofanescu, V. Babin, *Stimulated Brillouin Scattering: Fundamentals and Applications*, CRC Press, Boca Raton (2010)
7. Y. Wang, Z. Lu, W. He, Z. Zheng, Y. Zhao, A new measurement of stimulated Brillouin scattering phase conjugation fidelity for high pump energies. Laser Part. Beams **27**, 297–302 (2009)
8. D. Lin, H. Gao, Z. Lü, S. Wang, X. Zhao, Dependence of stimulated Brillouin scattering on the bandwidth, mode number, and mode separation of a laser, in *Advanced Laser Technologies 2005*, pp. 63441G-63441G-6 (2006)
9. W. Xiao-Hui, L. Zhi-Wei, L. Dian-Yang, W. Chao, Z. Xiao-Yan, T. Xiu-Zhang et al., Investigation of stimulated Brillouin scattering for broadband KrF laser. Chin. Phys. **13**, 1733–1737 (2004)

10. F. Starikov, G. Kochemasov, Novel phenomena at stimulated Brillouin scattering of vortex laser beams. Opt. Commun. **193**, 207–215 (2001)

11. H.S. Kim, D.-K. Ko, G. Lim, B.H. Cha, J. Lee, The influence of laser gain on stimulated Brillouin scattering in an active medium. Opt. Commun. **167**, 165–170 (1999)

12. D.A. Rockwell, A review of phase-conjugate solid-state lasers. IEEE J. Quantum Electron. **24**, 1124–1140 (1988)

13. M.C. Gower, R.G. Caro, phase conjugation of KrF laser radiation. Le Journal de Physique Colloques **44**, C2-19-C2-25 (1983)

14. A. Offenberger, M. Cervenan, A. Yam, A. Pasternak, Stimulated Brillouin scattering of CO2 laser radiation from underdense plasma. J. Appl. Phys. **47**, 1451–1458 (1976)

15. D.T. Hon, Pulse compression by stimulated Brillouin scattering. Opt. Lett. **5**, 516–518 (1980)

16. Z. Liu, Y. Wang, Z. Bai, Y. Wang, D. Jin, H. Wang et al., Pulse compression to one-tenth of phonon lifetime using quasi-steady-state stimulated Brillouin scattering. Opt. Express **26**, 23051–23060 (2018)

17. I. Velchev, D. Neshev, W. Hogervorst, W. Ubachs, Pulse compression to the subphonon lifetime region by half-cycle gain in transient stimulated Brillouin scattering. Quantum Electron. IEEE J. **35**, 1812–1816 (1999)

18. Y. Wang, X. Zhu, Z. Lu, H. Zhang, Generation of 360 ps laser pulse with 3 J energy by stimulated Brillouin scattering with a nonfocusing scheme. Opt. Express **23**, 23318–23328 (2015)

19. H. Yoshida, T. Hatae, H. Fujita, M. Nakatsuka, S. Kitamura, A high-energy 160-ps pulse generation by stimulated Brillouin scattering from heavy fluorocarbon liquid at 1064 nm wavelength. Opt. Express **17**, 13654–13662 (2009)

20. M. Jaberi, P. Jamshidi, S. Panahibakhsh, Control of SBS pulse compression by interaction geometrical parameters. Optics Commun. **530**, 129194 (2022)

21. S. Schiemann, W. Ubachs, W. Hogervorst, Efficient temporal compression of coherent nanosecond pulses in a compact SBS generator-amplifier setup. Quantum Electron. IEEE J. **33**, 358–366 (1997)

22. R. Menzel, H.J. Eichler, Temporal and spatial reflectivity of focused beams in stimulated Brillouin scattering for phase conjugation. Phys. Rev. A **46**, 7139–7149 (1992)

23. Y. Wang, W. Zhang, Y. Huang, J. Peng, Stimulated Brillouin scattering slow light in high nonlinearity silica microstructure fiber. Opt. Fiber Technol. **15**, 1–4 (2009)

24. V. Kovalev, N. Kotova, R. Harrison, "Slow Light" in stimulated Brillouin scattering: on the influence of the spectral width of pump radiation on the group index. Opt. Express **17**, 17317–17323 (2009)

25. Z. Shi, A. Schweinsberg, J.E. Vornehm, M.A.M. Gámez, R.W. Boyd, Low distortion, continuously tunable, positive and negative time delays by slow and fast light using stimulated Brillouin scattering. Phys. Lett. A **374**, 4071–4074 (2010)

26. Z. Zhu, W. Gao, C. Mu, H. Li, Reversible orbital angular momentum photon–phonon conversion. Optica **3**, 212–217 (2016)

27. H. Li, B. Zhao, L. Jin, D. Wang, W. Gao, Flat gain over arbitrary orbital angular momentum modes in Brillouin amplification. Photonics Res. **7**, 748–753 (2019)

28. H. Li, B. Zhao, J. Ni, W. Gao, Tailoring spatial structure of Brillouin spectra via spiral phase precoding. Photonics Res **9**, 637–642 (2021)

29. C. She, G. Herring, H. Moosmüller, S. Lee, Stimulated Rayleigh-Brillouin gain spectroscopy in pure gases. Phys. Rev. Lett. **51**, 1648 (1983)

30. C.W. Ballmann, J.V. Thompson, A.J. Traverso, Z. Meng, M.O. Scully, V.V. Yakovlev, Stimulated Brillouin scattering microscopic imaging. Sci. Rep. **5**, 18139 (2015)

31. D.L. Carroll, R. Johnson, S.J. Pfeifer, R.H. Moyer, Experimental investigations of stimulated Brillouin scattering beam combination. JOSA B **9**, 2214–2224 (1992)

32. H. J. Kong, J. W. Yoon, D. W. Lee, Beam combination using stimulated Brillouin scattering phase conjugate (2006)

33. H.J. Kong, J.W. Yoon, J.S. Shin, D.H. Beak, Long-term stabilized two-beam combination laser amplifier with stimulated Brillouin scattering mirrors. Appl. Phys. Lett. **92**, 021120--021120-3 (2008)

34. H.J. Kong, J.S. Shin, D.H. Beak, S. Park, J.W. Yoon, Current trends in laser fusion driver and beam combination laser systems using stimulated Brillouin scattering phase conjugate mirrors for a fusion driver. JKPS **56**, 177–183 (2010)

35. X. Xu, C. Feng, J.-C. Diels, Optimizing sub-ns pulse compression for high energy application. Opt. Express **22**, 13904–13915 (2014)

36. A.I. Erokhin, I.V. Smetanin, Experimental and theoretical study of self-phase modulation in sbs compression of high-power laser pulses. J. Russ. Laser Res. **31**, 452–461 (2010)

37. R. Chu, M. Kanefsky, J. Falk, Numerical study of transient stimulated Brillouin scattering. J. Appl. Phys. **71**, 4653–4658 (1992)

38. M. Jaberi, A. Farahbod, H.R. Soleimani, Effect of pump mode structure on reflectance of SBS mirrors. Opt. Quant. Electron. **49**, 53 (2017)

39. M. Jaberi, A.H. Farahbod, H. Rahimpur Soleimani, Spectral behavior of phase conjugated mirror in a two-pass optical amplifier. Iran. J. Phys. Res. **15**, 71–79 (2015)

40. M. Jaberi, A. Farahbod, H.R. Soleimani, Spectral behavior of amplified back-scattered Stokes pulse in two-cell phase conjugating mirror. Opt. Commun. **335**, 7–15 (2015)

41. V.A. Gorbunov, S. Papernyǐ, V. Petrov, V. Startsev, Time compression of pulses in the course of stimulated Brillouin scattering in gases. Sov. J. Quantum Electron. **13**, 900 (1983)

42. E. Hagenlocker, R. Minck, W. Rado, Effects of phonon lifetime on stimulated optical scattering in gases. Phys. Rev. **154**, 226 (1967)

43. V.I. Kovalev, V. Popovichev, V.V. Ragul'skii, F. Faizullov, Gain and line width in stimulated Brillouin scattering in gases. Sov. J. Quantum Electron. **2**, 69 (1972)

44. A. Kummrow, H. Meng, Pressure dependence of stimulated Brillouin backscattering in gases. Opt. Commun. **83**, 342–348 (1991)
45. M. Damzen, M. Hutchinson, W. Schroeder, Direct measurement of the acoustic decay times of hypersonic waves generated by SBS. IEEE J. Quantum Electron. **23**, 328–334 (1987)
46. M. Damzen, M. Hutchinson, High-efficiency laser-pulse compression by stimulated Brillouin scattering. Opt. Lett. **8**, 313–315 (1983)